

## Supporting Information

### Synthesis of Analogues Urchined Rutile Titania Carbon Nanocomposites by Iron-facilitated Phase Transformation of MXene for Environmental Remediation

*Guodong Zou<sup>1</sup>, Jianxin Guo<sup>1</sup>, Qiuming Peng<sup>1,\*</sup>, Qingrui Zhang<sup>2,\*</sup>, Aiguo Zhou<sup>3</sup> and Baozhong Liu<sup>3</sup>*

<sup>1</sup>State Key Laboratory of Metastable Materials Science and Technology, Yanshan University, Qinhuangdao, 066004, PR. China,

<sup>2</sup>Hebei Key Laboratory of Applied Chemistry, School of Environmental and Chemical Engineering, Yanshan University, Qinhuangdao, 066004, PR. China,

<sup>3</sup>School of Materials Science and Engineering, Henan Polytechnic University, Jiaozuo, 454000, PR. China

\* Corresponding author. Tel.: +86-335-8057047; fax: +86-335-8074545

E-mail address: pengqiuming@gmail.com; zhangqr@ysu.edu.cn

**Table S1.** The summarized Cr(VI) removal capacity, mechanism and condition of TiO<sub>2</sub> materials reported previously

TiO <sub>2</sub> crystal	Cr(VI) removal capacity	mechanism	Conditions	Reference
Mesoporous TiO <sub>2</sub> (anatase)	33.2mg/g	Adsorption	pH=6-8, 298K	S1
Amorphous hydrous TiO <sub>2</sub>	4.8 mg/g	Adsorption	pH=2	S2
TiO <sub>2</sub> -MCM-41 (anatase)	6.24mg/g	Adsorption	NA	S3
C/TiO <sub>2</sub> hybrid microsphere	18.1mg/g	Adsorption	pH=7, 298K	S4
Fe <sub>3</sub> O <sub>4</sub> @mTiO <sub>2</sub> @GO microspheres	67.3 mg/g	Adsorption	pH=2, 303K	S5
Anatase TiO <sub>2</sub> hollow spheres	23 mg/g	Adsorption	pH=2.7, 298K	S6
High surface area TiO <sub>2</sub> (anatase)	6.98 mg/g	Adsorption	NA	S7
Peroxide-modified TiO <sub>2</sub> (anatase)	63.5 mg/g	Adsorption	pH=5.0	S8
TiO <sub>2</sub> superstructure with ultrathin rutile nanorods	1000 mg/g	Photocatalysis	Sunlight for 3h	S9
Sulfated TiO <sub>2</sub> (anatase)	3.55 mg/g	Adsorption + Photocatalysis	NA	S10
Hierarchical structure	50 mg/g	Photocatalysis	4 h of UV irradiation	S11
TiO <sub>2</sub> hollow spheres				
<b>u-RTC</b>	<b>225 mg/g</b>	<b>Adsorption</b>	<b>pH= 5.8-6.5, 298K</b>	<b>Present study</b>

## References

- S1 Asuha, S.; Zhou, X.; Zhao, S. Adsorption of methyl orange and Cr (VI) on mesoporous TiO<sub>2</sub> prepared by hydrothermal method. *J. Hazard. Mater.* 2010, 181, 204-210.
- S2 Tel, H.; Altaş, Y.; Taner, M. Adsorption characteristics and separation of Cr (III) and Cr (VI) on hydrous titanium (IV) oxide. *J. Hazard. Mater.* 2004, 112, 225-231.
- S3 Parida, K.; Mishra, K. G.; Dash, S. K. Adsorption of toxic metal ion Cr(VI) from aqueous state by TiO<sub>2</sub>-MCM-41: Equilibrium and kinetic studies. *J. Hazard. Mater.* 2012, 241–242, 395-403.
- S4 Qian, H.; Hu, Y.; Liu, Y.; Zhou, M.; Guo, C. Electrostatic self-assembly of TiO<sub>2</sub> nanoparticles onto carbon spheres with enhanced adsorption capability for Cr(VI). *Mater. Lett.* 2012, 68, 174-177.
- S5 Li, L.; Duan, H.; Wang, X.; Luo, C. Adsorption property of Cr (VI) on magnetic mesoporous titanium dioxide-graphene oxide core-shell microspheres. *New J. Chem.* 2014, 38, 6008-6016.
- S6 Xiang, W. C.; Hu, P.; Zhang, X.; Yao, M. S.; Xu, R. F.; Yuan, F. L. Synthesis of Porous TiO<sub>2</sub> Hollow Spheres by Hydrothermal Method and Their Adsorption Property to Cr (VI). *Chin. J. Process Eng.* 2011, 4, 024.
- S7 Vassileva, E.; Hadjiivanov, K.; Stoychev, T.; Daiev, C. Chromium speciation analysis by solid-phase extraction on a high surface area TiO<sub>2</sub>. *Analyst* 2000, 125, 693-698.
- S8 Vasileva, E.; Mandjukova, K. H. Adsorption of Cr<sup>6+</sup> oxo anions on pure and peroxide-modified TiO<sub>2</sub> (anatase). *Colloids Surf. A Physicochem. Eng. Asp.* 1994, 90, 9-15.
- S9 Xing, Y.; Chen, X.; Wang, D. Electrically regenerated ion exchange for removal and recovery of Cr (VI) from wastewater. *Environ. Sci. Technol.* 2007, 41, 1439-1443.
- S10 Jiang, F.; Zheng, Z.; Xu, Z.; Zheng, S.; Guo, Z.; Chen, L. Aqueous Cr (VI) photo-reduction catalyzed by TiO<sub>2</sub> and sulfated TiO<sub>2</sub>. *J. Hazard. Mater.* 2006, 134, 94-103.

S11 Yang, Y.; Wang, G.; Deng, Q.; Wang, H.; Zhang, Y.; Ng, D. H.; Zhao, H. Enhanced photocatalytic activity of hierarchical structure TiO<sub>2</sub> hollow spheres with reactive (001) facets for the removal of toxic heavy metal Cr (VI). *RSC Advances* 2014, 4, 34577-34583.

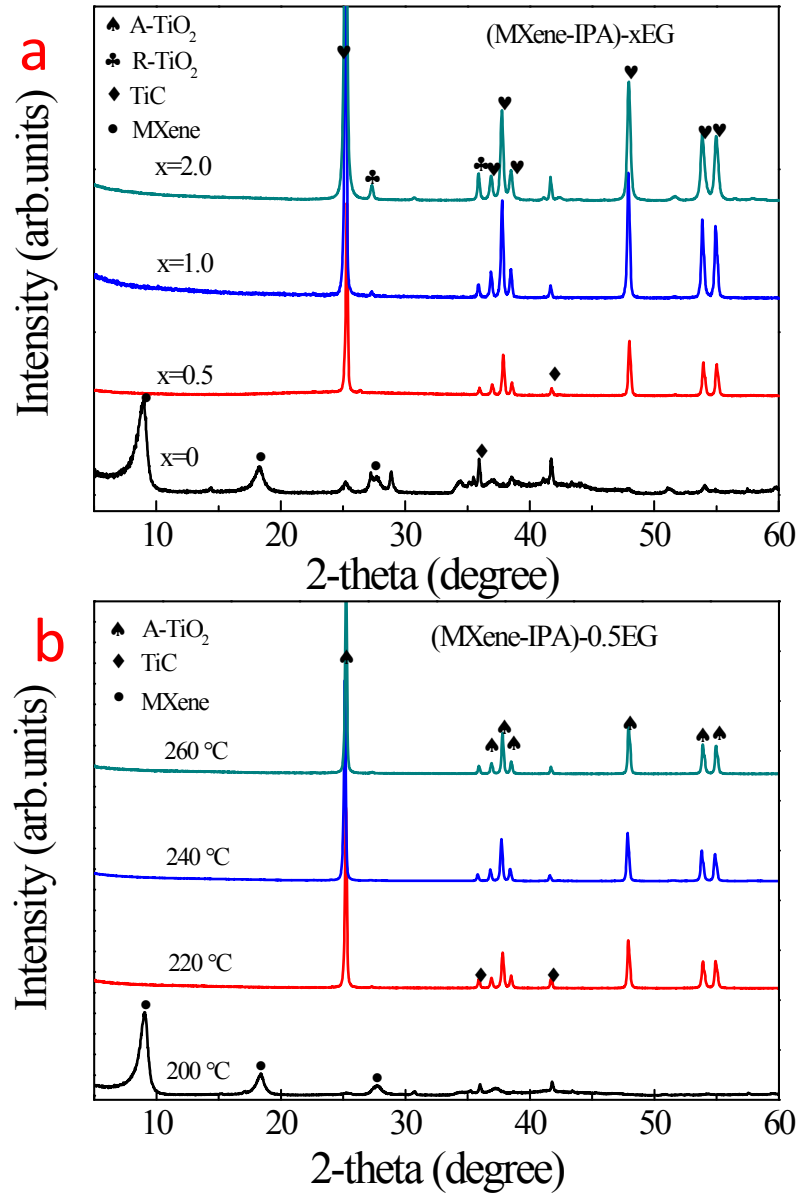


**Figure S1.** XRD patterns of different samples. (a) at 220°C under different EG concentrations; (b) at different temperatures with 0.5EG.

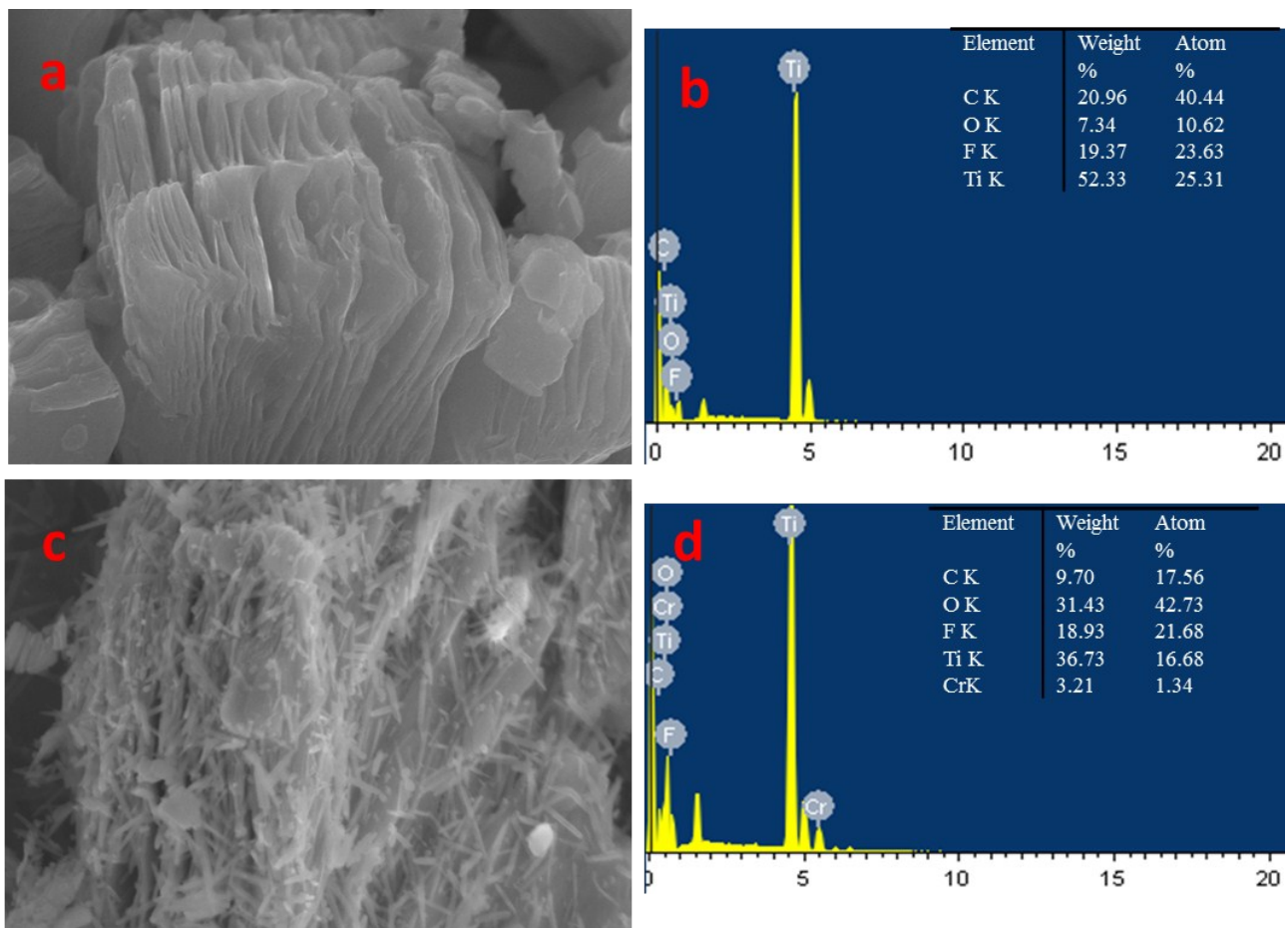


**Figure S2.** (a) and (b) The morphology of MXene and its chemical composition, respectively. (c) and (d) The morphology of u-RTC after removing Cr and its chemical composition, respectively.

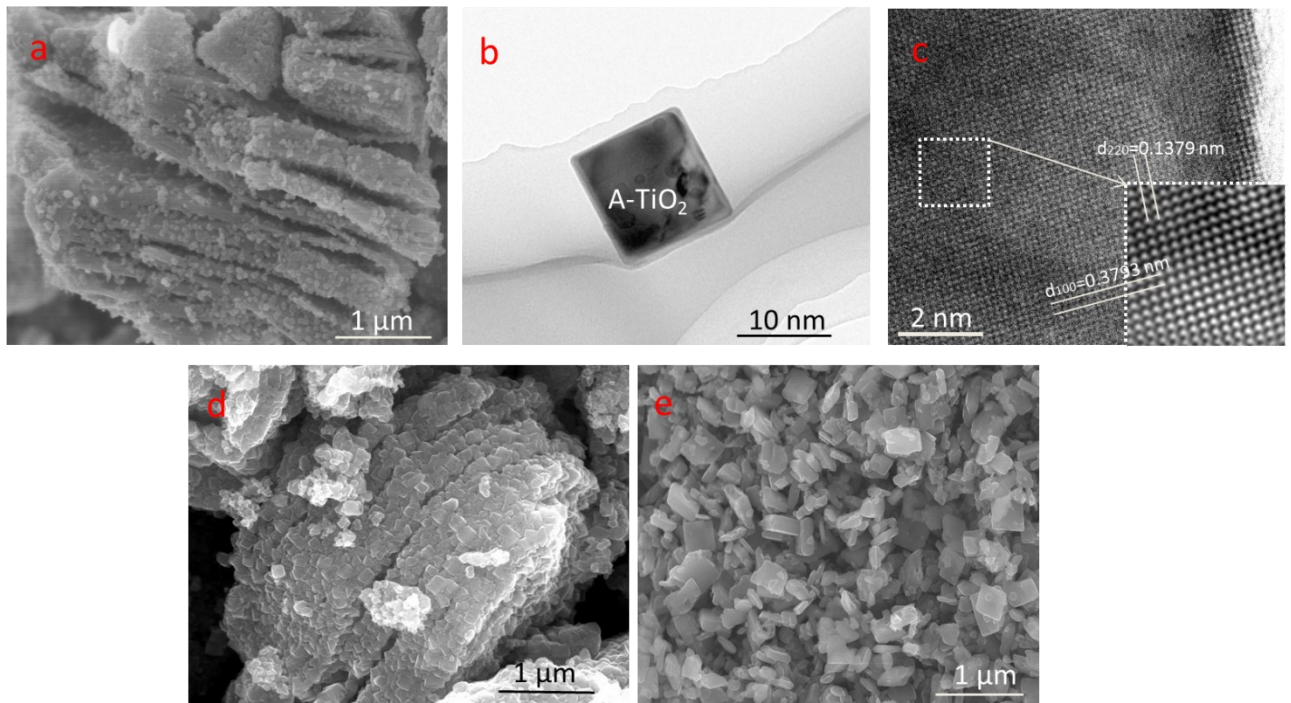


**Figure S3.** The morphology variation during decomposition of MXene at 220 °C. (a) The SEM image of (MXene-IPA)-0.5EG for 1 h. (b) and (c) The TEM and HRTEM images of (MXene-IPA)-0.5EG for 1 h, respectively. (d) The SEM image of (MXene-IPA)-0.5EG for 4 h. (e) The SEM image of (MXene-IPA)-0.5EG for 24 h.

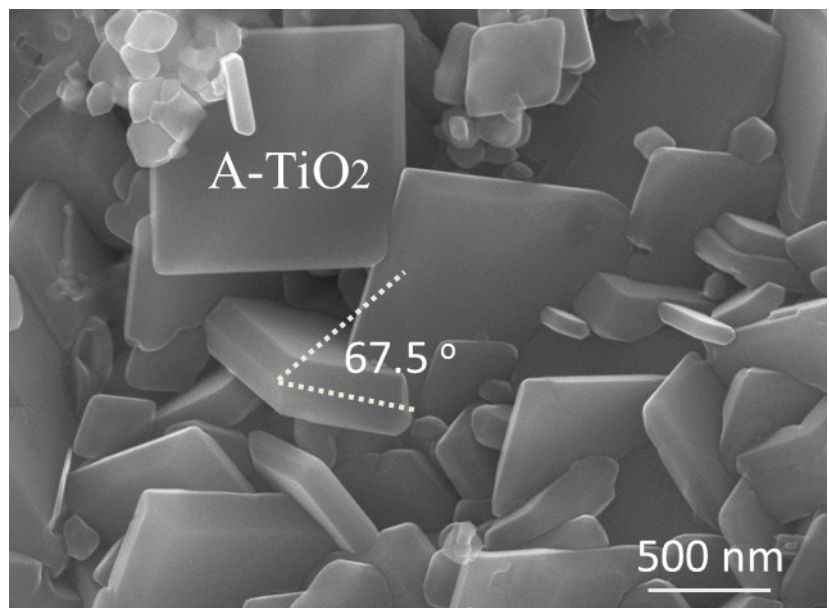


**Figure S4.** The SEM image of (MXene-IPA)-0.5EG for 28 h, which is similar to that of 24 h. The white dash lines indicate the (001) and (101) crystal planes of A-TiO<sub>2</sub>, respectively. The angle is  $67.5 \pm 0.5^\circ$  on average.

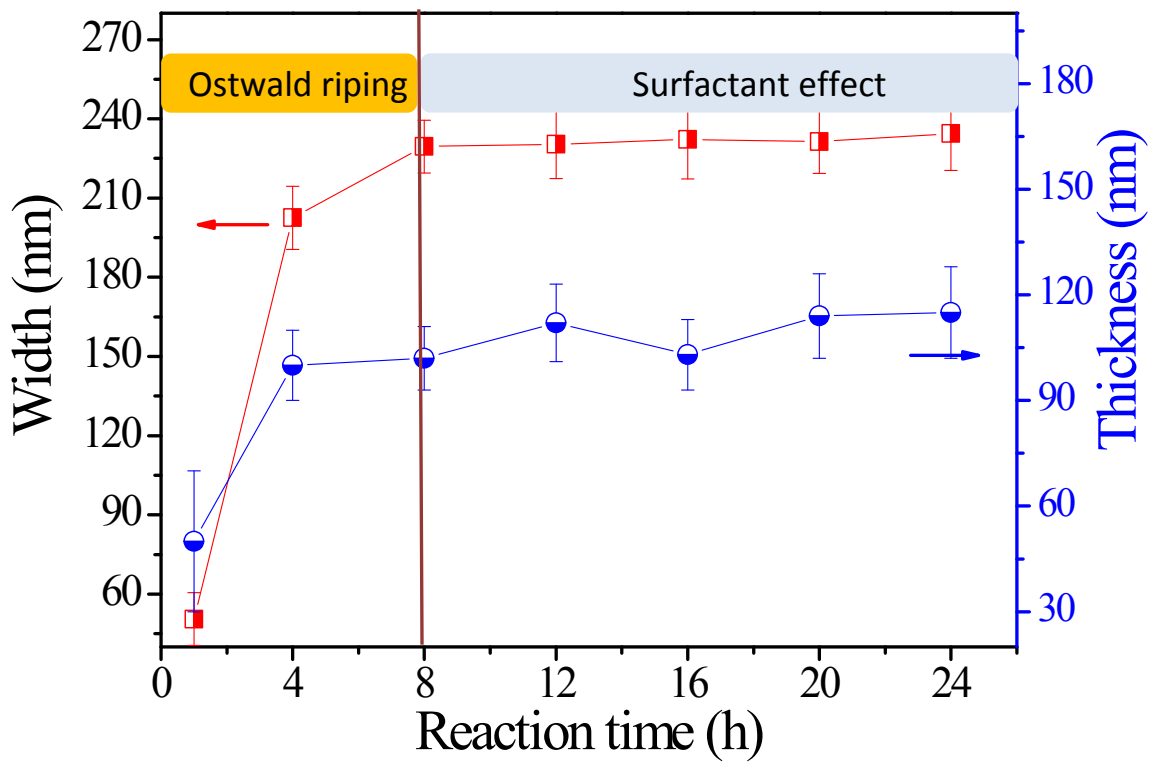


**Figure S5.** The effect of reaction time on the width and thickness of anatase  $\text{TiO}_2$  in (MXene-IPA)-0.5EG.

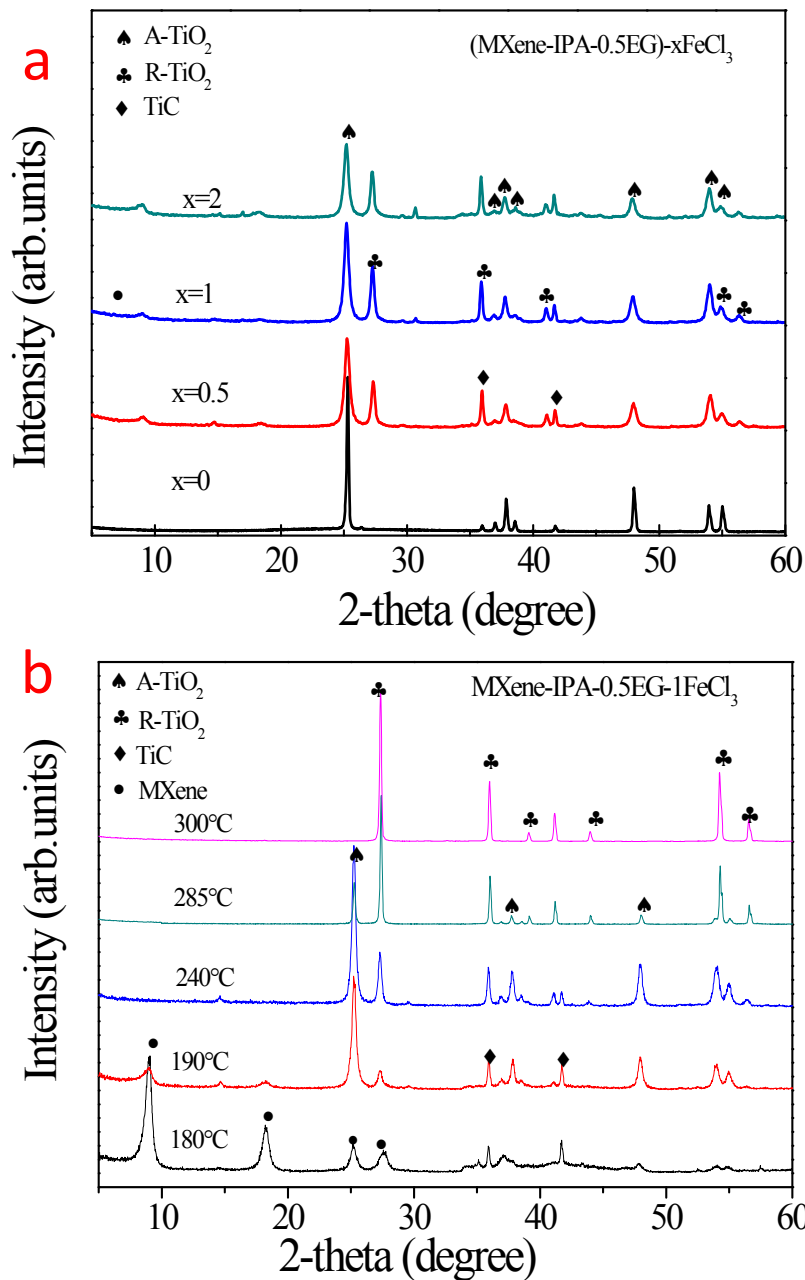


**Figure S6.** The representative XRD patterns. (a) The effect of  $\text{FeCl}_3$  concentrations on the phase composition of decomposed MXene at 220 °C for 24 h. (b) The effect of reaction temperatures on the phase composition of decomposed MXene with 0.5EG for 24 h.

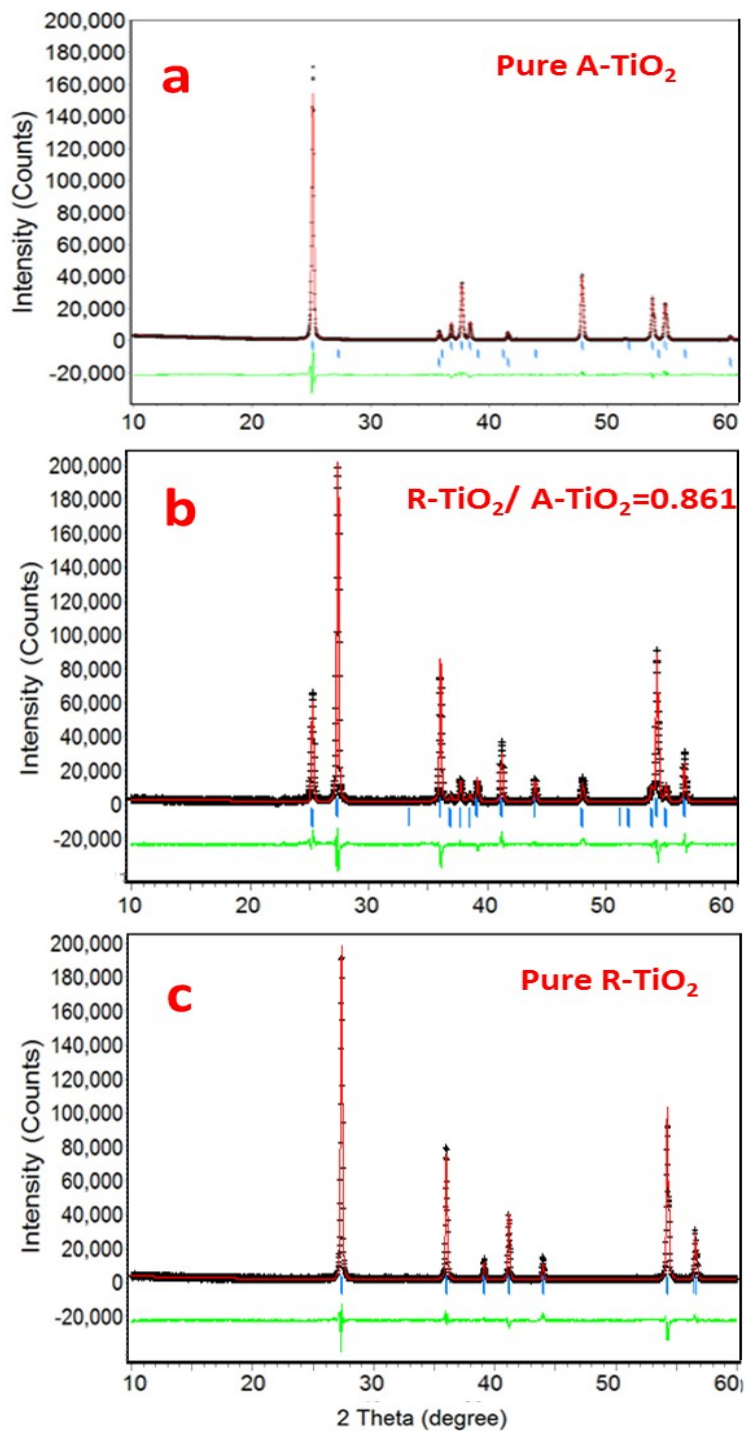


**Figure S7.** The typical Rietveld refinement graphs (Fullprof software) of the samples, (a) IPA+0.5EG at 300 °C for 24 h, (b) IPA+0.5EG+1FeCl<sub>3</sub> at 220 °C for 24 h. (c) IPA+0.5EG+1FeCl<sub>3</sub> at 300 °C for 24 h.

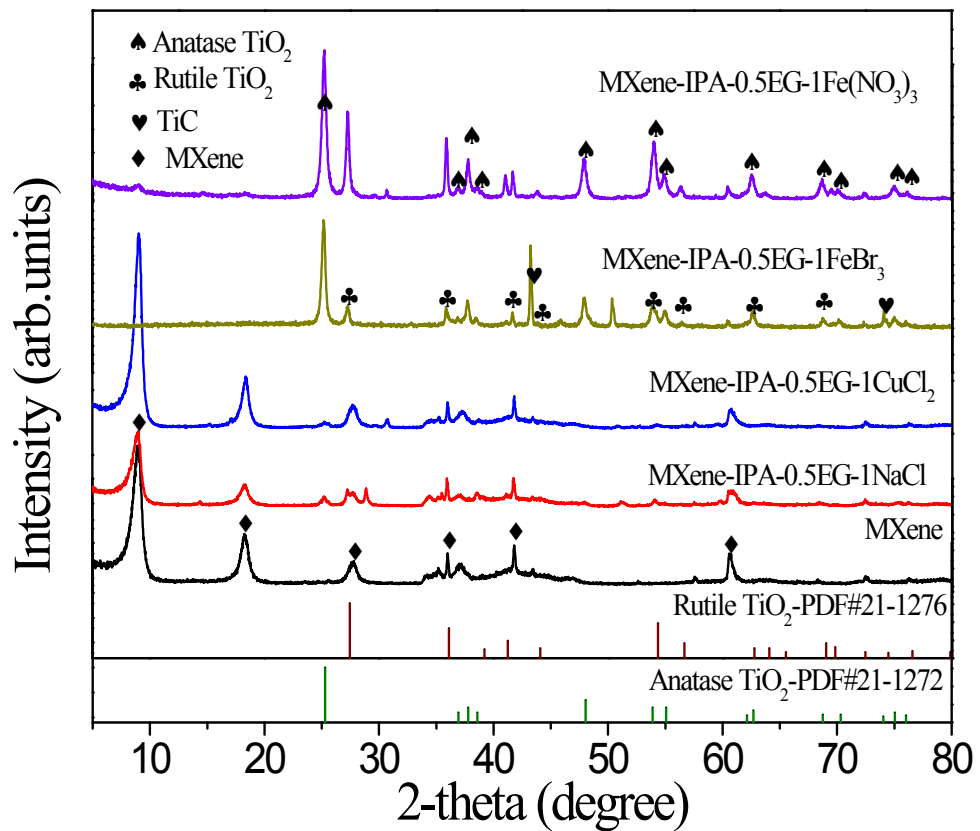


**Figure S8.** The effect of salts on the phase transformation of MXene at 220 °C for 24 h

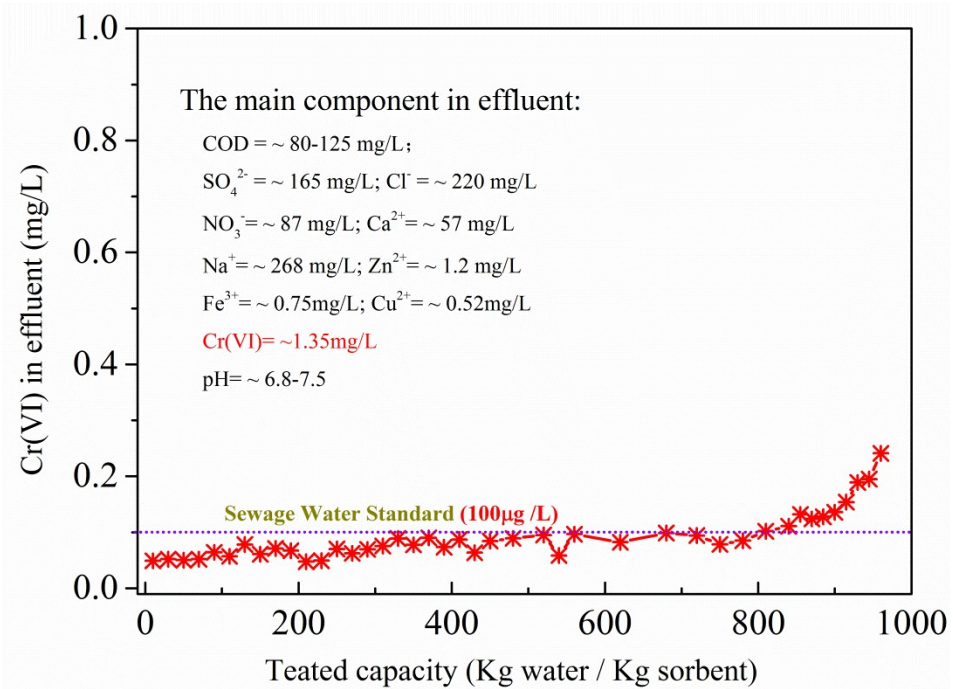


**Figure S9** The real wastewater verification towards Cr(VI) removal. Note that the samples were got from the effluent of electroplating wastewater for further purification with the help of HaoYuan Environmental Engineering Co. China.

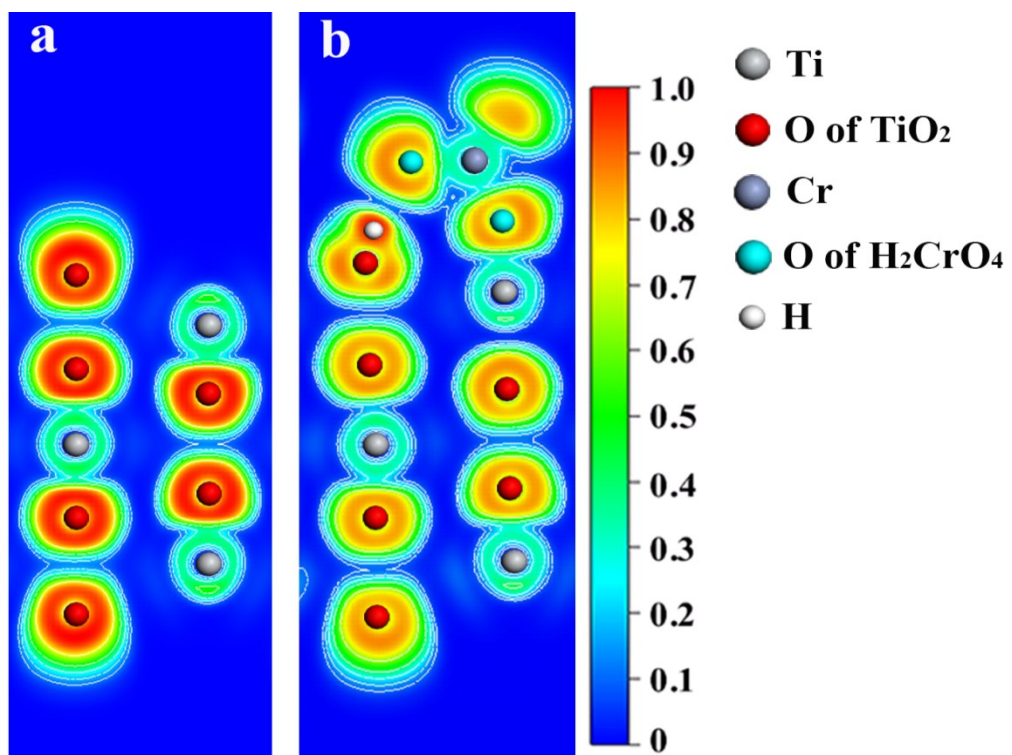


**Figure S10** ELFs of R-TiO<sub>2</sub>(110) surface (a) and H<sub>2</sub>CrO<sub>4</sub> adsorption on R-TiO<sub>2</sub>(110) surface (b).

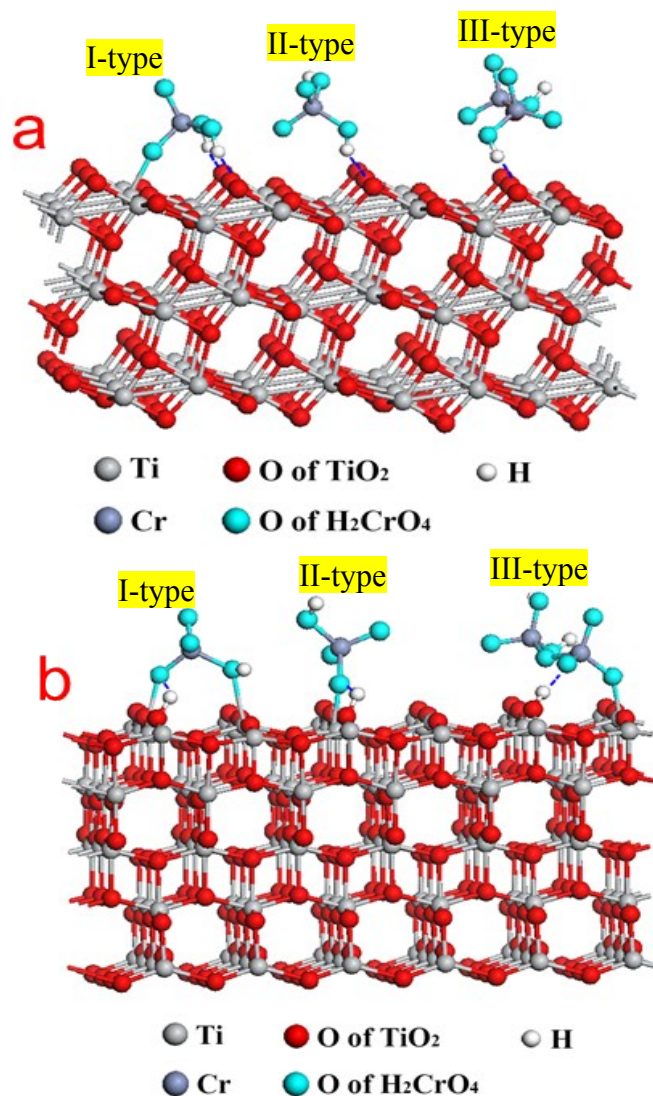


**Figure S11.** The adsorption sketch map of  $\text{CrO}_4^{2-}$  (I-type),  $\text{HCrO}_4^-$  (II-type), and  $\text{Cr}_2\text{O}_7^{2-}$  (III-type) ions using the different adsorption structures of  $\text{H}_2\text{CrO}_4$  and  $\text{H}_2\text{Cr}_2\text{O}_7$ , respectively. a) A- $\text{TiO}_2$  (101) surface b) A- $\text{TiO}_2$  (001) surface.

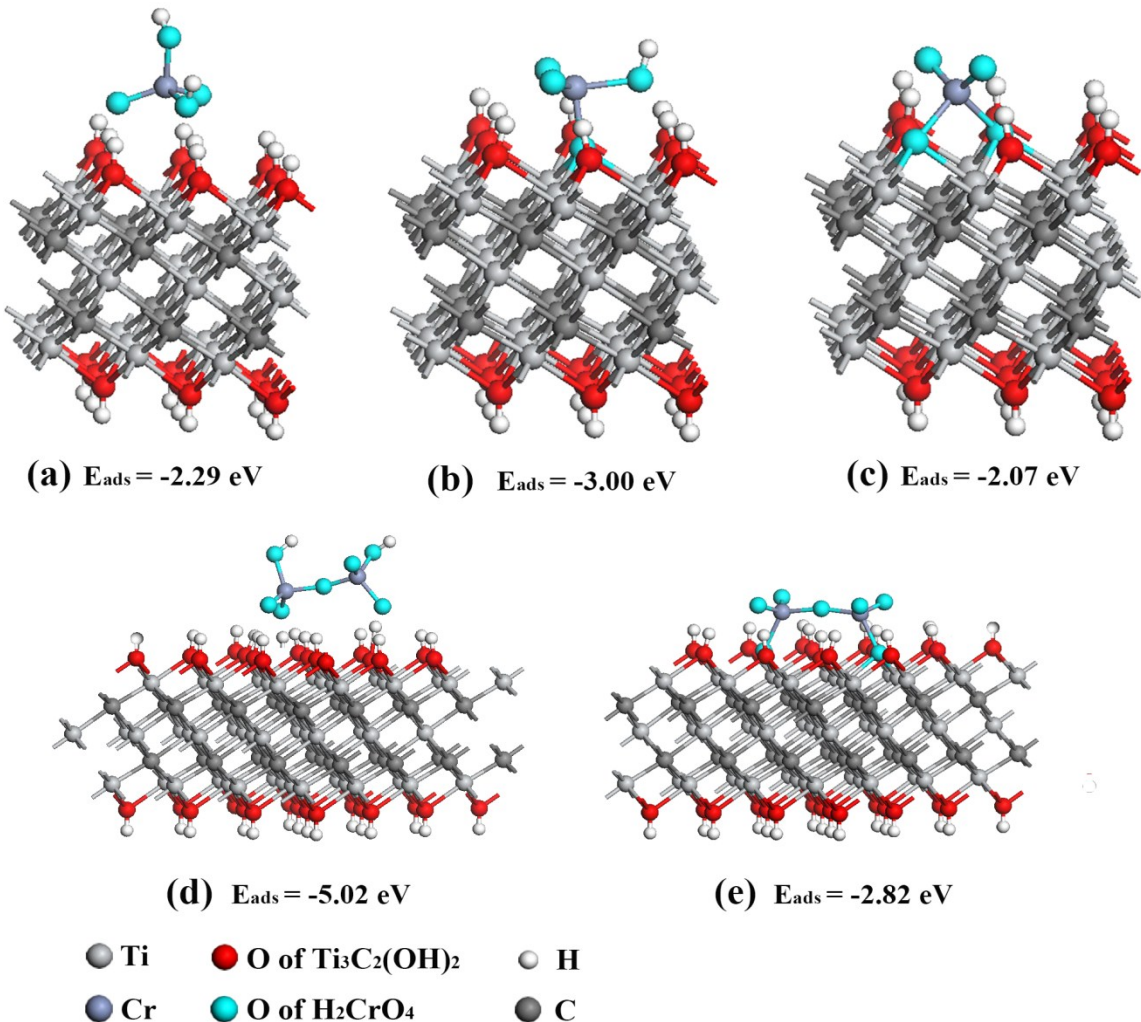


**Figure S12** The sketch map and adsorption energies or formation energies of  $\text{H}_2\text{CrO}_4$  and  $\text{H}_2\text{Cr}_2\text{O}_7$  adsorption on  $\text{Ti}_3\text{C}_2(\text{OH})_2$  surface. (a) electrostatic adsorption of  $\text{H}_2\text{CrO}_4$ ; the chemical adsorption by the formation of one (b) or two  $\text{H}_2\text{O}$  (c) coming from  $\text{OH}^-$  of  $\text{Ti}_3\text{C}_2(\text{OH})_2$  and  $\text{H}^-$  of  $\text{H}_2\text{CrO}_4$ ; (d) electrostatic adsorption of  $\text{H}_2\text{Cr}_2\text{O}_7$ ; (e) the chemical adsorption by the formation of one  $\text{H}_2\text{O}$  coming from  $\text{OH}^-$  of  $\text{Ti}_3\text{C}_2(\text{OH})_2$  and  $\text{H}^-$  of  $\text{H}_2\text{Cr}_2\text{O}_7$ .